Sensitivity Analysis for Energy Demand Estimation of Electric Vehicles

Johannes Asamer[a,*], Anita Graser[a], Bernhard Heilmann[a], Mario Ruthmair[b]

[a] *Mobility Department, Austrian Institute of Technology, Donau City Straße 1, 1220, Vienna, Austria*
[b] *Department of Statistics and Operations Research, University of Vienna, Austria*

Abstract

We present a sensitivity analysis for a mechanical model, which is used to estimate the energy demand of battery electric vehicles. This model is frequently used in literature, but its parameters are often chosen incautiously, which can lead to inaccurate energy demand estimates. We provide a novel prioritization of parameters and quantify their impact on the accuracy of the energy demand estimation, to enable better decision making during the model parameter selection phase. We furthermore determine a subset of parameters, which has to be defined, in order to achieve a desired estimation accuracy. The analysis is based on recorded GPS tracks of a battery electric vehicle under various driving conditions, but results are equally applicable for other BEVs. Results show that the uncertainty of vehicle efficiency and rolling friction coefficient have the highest impact on accuracy. The uncertainty of power demand for heating and cooling the vehicle also strongly affects the estimation accuracy, but only at low speeds. We also analyze the energy shares related to each model component including acceleration, air drag, rolling and grade resistance and auxiliary energy demand. Our work shows that, while some components make up a large share of the overall energy demand, the uncertainty of parameters related to these components does not affect the accuracy of energy demand estimation significantly. This work thus provides guidance for implementing and calibrating an energy demand estimation based on a longitudinal dynamics model.

Keywords: energy demand, electric vehicles, sensitivity analysis

1. Introduction

Battery electric vehicles (BEVs) have the potential to significantly reduce oil dependency, decrease carbon emissions and noise, avoid tail pipe emissions and increase energy efficiency of transportation. Several car manufacturers have released new types of BEVs and in many European countries the charging infrastructure for BEVs is constantly expanded. Additionally, funding programs and research activities have been started, aiming at improving different aspects

*Corresponding author
Email addresses: johannes.asamer@ait.ac.at (Johannes Asamer), anita.graser@ait.ac.at (Anita Graser), bernhard.heilmann@ait.ac.at (Bernhard Heilmann), mario.ruthmair@univie.ac.at (Mario Ruthmair)

of electric mobility. Experts are confident that in the near future BEVs will achieve a significant market penetration (Situ, 2009).

Regarding energy efficiency of driving (tank to wheel efficiency), a BEV performs much better than an internal combustion engine vehicle (ICEV). It is worth noting that this does not include the energy efficiency of fuel production or electricity generation, which varies significantly depending on the mix of energy sources that are available in a certain region or country. Given a high efficiency of energy production, the overall efficiency (well to wheel) of BEVs can be up to twice the overall efficiency of ICEV (Kromer and Heywood, 2007).

A reason for the better tank to wheel efficiency of a BEV is the higher efficiency of the electric motor (up to 95% (EVO Electric, 2014)) compared to a combustion engine (up to 35% for gasoline fuels (Treiber and Kesting, 2010)). Electric motors are able to provide a high torque for a broad range of rotational speeds. Therefore only a single gear transmission is needed, which further increases the efficiency of the drive train. In general, a BEV contains fewer moving and rotating parts than an ICEV, resulting in lower maintenance costs (Kampker et al., 2013; Pelletier et al., 2014). Energy efficiency is further increased by the ability of the electric motor to act as a generator. During decelerating and driving downhill, energy can be transformed into electric energy and transferred back to the battery, instead of being dissipated by friction brakes.

Although energy efficiency of BEVs is high, their driving range without charging is much shorter than typical ICEV driving ranges. Currently available BEVs reach driving distances of approximately 150km with a fully charged battery. Among BEVs, the largest driving range of approximately 420km is possible with the Tesla Model S, equipped with a 85kWh battery. In contrast, an average ICEV can easily cover a distance of 800km and more with one tank of gasoline. The situation is aggravated by very hot or cold ambient temperatures, which increase the energy demand for cooling or heating.

The reason for short driving ranges is the relatively small amount of energy that can be stored in the battery. A battery has a much lower specific energy (energy capacity per unit mass) than a fossil fuel. Nowadays, lithium-ion batteries, as used in the automotive industry, achieve a specific energy of up to 130Wh/kg, but specific energy of gasoline is approximately ten times higher (1233Wh/kg, (Young et al., 2013)). Other battery types currently used in BEVs (Ni-MH, Zebra) do not achieve higher specific energy values than lithium-ion batteries. Moreover the price (in costs per capacity) of a standard lithium-ion battery is about 250USD/kWh (Young et al., 2013; Pelletier et al., 2014). Building larger batteries for larger driving distances would therefore increase price and weight of the vehicle. Additional weight also means increased energy consumption and reduced efficiency. Therefore, it is a challenge for car manufactures to find a good trade-off between driving range, price and weight.

Because of the small energy storage capability of batteries, it is necessary to know, how much energy is consumed by the BEV, in order to estimate the maximum driving range. In the literature, a model, which describes the vehicle behaviour based on the general principles of mechanics, is often used to estimate the (electric) energy demand. We refer to this model as longitudinal dynamics model (LDM), because it describes the movement behaviour of a vehicle along its longitudinal direction. An LDM contains several parameters related to properties of the vehicle and its environment. The literature provides various references for setting parameters to specific values. Due to varying in-

dications in the literature and different properties of environment and vehicles, all model parameters are subject to uncertainty within a certain range, which causes a variation in energy consumption estimation. The question is, which of the model parameter uncertainties have a higher influence on the accuracy of the energy consumption estimation and therefore have to be configured more thoroughly. The answer to this question is also relevant for finding measures to reduce the energy consumption. This paper aims at analyzing the sensitivity of the LDM and thus the BEV's energy consumption. Moreover, the composition of the total energy estimate, based on the individual LDM components, is investigated.

The key contribution of this paper is to assess the variance of energy consumption estimation due to the uncertainty of parameters of the LDM. A sensitivity analysis is carried out, in order to investigate the influence of individual parameters. The analysis is based on recorded GPS tracks of a BEV. The uncertainty of parameters is specifically determined for a Mitsubishi i-MiEV but is equally applicable for other BEVs.

Our analysis results provide a basis for LDM users to focus on important parameters, which need to be determined exactly, while assuming standard values for less important ones. Thus, the calibration of an LDM can be improved in terms of accuracy and performance, by using only the most important parameters, thus reducing parameter search space.

The remainder of the paper is organized as follows: In Section 2 we give a detailed description of the LDM and summarize different applications for the LDM found in literature. We describe the theory and application of sensitivity analysis in Section 3 and discuss the data base used for conducting the sensitivity analysis in Section 4. In Section 5 we perform a preliminary analysis regarding the energy shares related to each component of the LDM. Results are presented in Section 6. Conclusions are drawn in Section 7 including recommendations for users of the LDM and future research activities.

2. Longitudinal Dynamics Model

The movement behaviour of a vehicle along its moving direction is completely determined by all forces acting on it in this direction (Ehsani et al., 2009). Figure 1 shows the forces for a vehicle moving uphill. Air drag, rolling and grade resistance are the external forces. Tractive effort to overcome these forces and to accelerate has to be provided by the internal (electric) engine.

2.1. Definition

Firstly we give a description of the relation between external forces, acceleration and basic energy consumption. During a vehicle's movement, the external resistances are trying to stop it. According to Newton's second law, the relationship between forces and acceleration can be written as

$$F_T = \frac{dv}{dt} \cdot f \cdot m + F_R, \tag{1}$$

where F_T is the traction force, provided by the electric motor and F_R are the aforementioned resistances acting on the vehicle. The total vehicle mass is m and f is the mass factor of all rotating parts. In order to overcome resistance

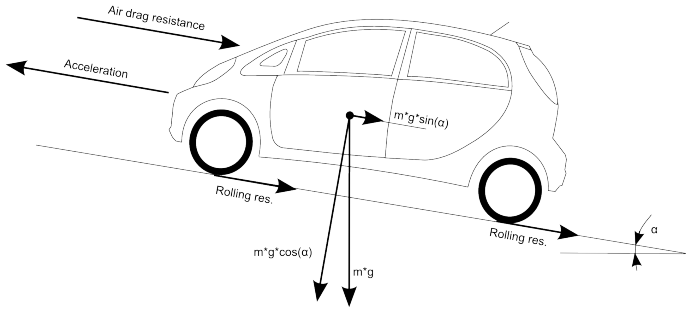

Figure 1: Forces acting on a vehicle moving uphill.

forces and to accelerate with $\frac{dv}{dt}$, the motor has to provide traction force. The composition of resistances is described as

$$F_R = \underbrace{m \cdot g \cdot sin(\alpha)}_{Grade} + \underbrace{m \cdot g \cdot cos(\alpha) \cdot c_{rr}}_{Rolling} + \underbrace{\frac{\rho \cdot A \cdot cw}{2} \cdot v^2}_{Air}, \tag{2}$$

where g is the gravitational acceleration, α the road gradient and c_{rr} the rolling friction coefficient. Air drag is influenced by velocity v, air density ρ, vehicle front surface area A and air drag coefficient cw. All parameters of the model are described in detail in Section 3.2.

The power required for driving is the traction force times the velocity of the vehicle. This mechanical power is provided by the electric motor, which draws electric energy from the battery. Considering efficiency rates, the electric power drawn from the battery is

$$P_{el,out} = \frac{F_T \cdot v}{\eta_M} + P_0, \tag{3}$$

where η_M is the energy efficiency of transmission, motor and power conversion. Auxiliary components of the car are causing an additional demand of electric power, denoted as P_0. This value depends mainly on the usage of heating or air condition and already contains an efficiency rate. During deceleration or driving downhill, traction force F_T may be negative and energy is transmitted back to the battery. In this case, the motor is acting as a generator. This situation is called recuperation and can be described by

$$P_{el,in} = \begin{cases} 0 & \text{if } v \leq V_{min} \\ F_T \cdot v \cdot \eta_G + P_0 & \text{else} \end{cases}, \tag{4}$$

with η_G as the efficiency of transmission, generator and in-vehicle charger. Energy cannot be recuperated below V_{min}. Again, P_0 is the power demand of auxiliary components required for operating the vehicle. If the braking strength is less than 0.2 times the gravity acceleration ($0.2g$), all the braking force is allocated to the wheels connected to the electric motor (Ehsani et al., 2009). Beyond this limit (e.g., for hard brakes), braking strength is distributed to all wheels in order to maintain driving stability. In this case, energy is dissipated by friction brakes and Eq. (4) would overestimate the recuperated energy. In the FTP75 Urban driving cycle, for example, all decelerations fall below $0.2g$

(Ehsani et al., 2009) and similarly, in the vehicle data used in this study (cf. Section 4) 98% of the decelerations are below this limit. Therefore, we argue that applying Eq. (4) is appropriate to estimate recuperated energy for a whole trip.

To estimate the total energy demand of a trip, all electrical in- and outflows have to be summarized by

$$E_{el} = \int_0^T P_{el}\ dt, \tag{5}$$

where T is the time duration of the trip and P_{el} can be either $P_{el,out}$ for driving or $P_{el,in}$ for recuperating and is defined as

$$P_{el} = \begin{cases} P_{el,out} & \text{if } F_T \geq 0 \\ P_{el,in} & \text{if } F_T < 0 \end{cases}. \tag{6}$$

2.2. Application

The model described in the previous section can be used for estimating instantaneous electric power (Eq. (3) and (4)) and energy consumption for a whole trip (Eq. (5)). Input data are vehicle trajectories, typically gathered by a GPS data recorder. Alternatively, a trajectory could be estimated for a predefined route, based on velocities, which can be derived from travel information services.

Trajectories must contain distance, speed and acceleration between consecutive locations, either measured directly or derived from other variables (e.g. acceleration from speed). To estimate the energy consumption of a trajectory, the integral of Eq. (5) is replaced by the sum over all elements of the trajectory. Thus Eq. (5) is rewritten as

$$E_{el} = \sum_{i=1}^{N} P_{el,i} \cdot \Delta t, \tag{7}$$

where Δt is the time span between two locations of the trajectory and N is its length. $P_{el,i}$ is the electric power estimated at each time step i according to Eq. (6). In order to compare different trips with varying mileage, we divide energy consumption by trip length and therefore we obtain energy per distance unit ($kWh/100km$). The energy consumption per distance is calculated by

$$EC = \frac{E_{el}}{L}, \tag{8}$$

where L is the length of the whole trajectory.

2.3. LDM in the Literature

In this section we provide an overview of the state of the art regarding energy demand estimation. Moreover we identify LDM applications and how the parameters of the respective model are chosen. From the literature, we can identify the following groups of LDM applications, which are discussed in more detail subsequently:

- Estimating energy consumption from either real world or simulated trajectory data (Wu et al., 2015; Hayes et al., 2011; Maia et al., 2011; Boubaker et al., 2013)

- Determining the influence of driving behaviour on energy demand (Frank et al., 2013; Araujo et al., 2012; Younes et al., 2013)
- Energy efficient routing and fleet optimization (Sachenbacher et al., 2011; Artmeier et al., 2010; Prandtstetter et al., 2013; Hiermann et al., 2015; Pelletier et al., 2014; Goeke and Schneider, 2015; Preis et al., 2014)
- Predicting expected energy demand and range estimation (Sehab et al., 2011; Vaz et al., 2015; Zhang et al., 2012; Ferreira et al., 2013)

Factors influencing energy demand of electric vehicles are investigated by Younes et al. (2013). They observe that driving style, different road types and ambient temperature have the highest effect on energy consumption. The impact of driving style on energy consumption is widely discussed, for example in Frank et al. (2013); Araujo et al. (2012). For individual trips, different indicators (e.g. arithmetic average) for speed, acceleration and jerk are used to describe driving style. Although in our study we also investigate impacts on energy consumption, driving behaviour is not considered in detail. The reasons behind this decision are described in the conclusion where we argue why the obtained results are not affected by the driving behaviour. Instead our approach is to examine the impact of vehicle parameters rather than driver influence. Driving behaviour is considered so far as the sensitivity analysis is performed with regards to different speeds.

Accuracy of the LDM is the topic of a study by Wu et al. (2015), where energy consumption is measured by a test vehicle and compared to an estimated energy consumption obtained from the LDM. Regarding motor efficiency they consider a more detailed description, based on current and motor resistance. The choice of parameter values is based on related literature, with no reference mentioned. Particularly the choice for the rolling friction coefficient, which is only 0.006, is remarkable, since higher values for the rolling friction coefficient are recommended (between 0.007 and 0.014) by the National Research Council (2006). The energy consumption is estimated for two specific electric vehicles (Nissan Leaf and Tesla Roadster) by applying an LDM by Hayes et al. (2011). The model is used for range estimation for a given driving cycle and results are compared to manufacturer specifications. For the Tesla Roadster, a rolling friction coefficient of only 0.0055 is assumed.

The open source microscopic traffic simulator SUMO is extended by Maia et al. (2011) to estimate the energy consumption of simulated BEVs. The LDM uses trajectories generated by the traffic simulation. All parameters of the LDM are chosen based on the EV1 electric vehicle produced by General Motors. Again a remarkably low rolling friction coefficient of 0.005 is chosen. Moreover, values for motor efficiencies are taken from a study analyzing hybrid electric vehicles. An LDM is applied to trajectories of a microscopic traffic simulation by Boubaker et al. (2013) to estimate the impact of hybrid electric vehicles on the energy consumption of all vehicles in the road network.

Sehab et al. (2011) apply an LDM to driving cycles (called mission profiles) to estimate required motor torque and energy consumption. Results are used to dimension the drive train of a BEV. Moreover, based on energy consumption of mission profiles, a simplified control strategy is implemented in the motor. Furthermore to estimate driving ranges, the energy demand has to be predicted.

This is done by Vaz et al. (2015), Zhang et al. (2012) and Ferreira et al. (2013) for a predicted speed profile.

The required tractive effort of a vehicle can be estimated by an LDM and is therefore applicable for ICEVs as well. One difference is that, for a combustion engine, efficiency varies more than for an electric motor and it strongly depends on the rotational speed of the motor, i.e. the chosen gear. Demir et al. (2011) use an LDM for estimating CO2 emissions of ICEVs, which are highly correlated to energy consumption. Also Treiber and Kesting (2010) propose an LDM for estimating fuel consumption, which is equivalent to energy consumption. Regarding the efficiency, they assume that the driver is choosing the optimal gear at each state. Therefore, the estimated fuel consumption is lower than in real world conditions.

With the introduction of electric vehicles and their relatively short driving ranges, methods emerged for finding the most energy efficient route. The problem consists of two main parts: estimating the energy consumption per road link and applying an appropriate routing algorithm (Pelletier et al., 2014). Again an LDM is used to obtain the energy consumption per road link, where a speed profile has to be assumed (Sachenbacher et al., 2011; Artmeier et al., 2010; Prandtstetter et al., 2013). For the routing algorithm, energy consumption is the weight assigned to each road link. Since, for BEV, energy consumption on some links can be negative (e.g. driving downhill), a classical Dijkstra-algorithm is only applicable for ICEVs or if recuperated energy is ignored. Otherwise alternative routing algorithms have to be developed (Abousleiman and Rawashdeh, 2014). Moreover, energy efficient routing can be formulated as multi-objective optimization problem, because travel time and energy consumption may contradict each other. For example, a low speed route could be more efficient than a highway due to higher air resistance at high speeds.

Although the LDM (with modifications) is prevalently used for estimating energy consumption of vehicles, there are alternatives. Terras et al. (2011) apply a vehicle model for energy estimation, which is more detailed than the LDM and integrates vehicle parameters like wheel radius and transmission ratio. A completely different modelling approach is chosen by Shankar and Marco (2013), namely a neural network, which is a machine learning method for modelling a non-linear relationship between several inputs and the output. Several trips are divided into a large number of microtrips of 30 seconds and the neural network is trained with these microtrips. 28 parameters of a microtrip describing, mainly speed and acceleration of the trajectory, are used as input to the neural network and the output is the measured energy consumption of the vehicle. The neural network is able to accurately predict energy estimation, but it requires training data. This approach is similar to the study of Diaz Alvarez et al. (2014), in which 14 features of individual trips are used to train a neural network in order to predict the energy consumption. Additionally, they perform a 'one at a time' analysis, where only one input feature is varied, while all others are fixed and the variability of the output is observed. Among features describing the driving behaviour they conclude that jerk has the highest influence.

2.4. LDM in our Study

In contrast to the existing literature, in our study, we are assessing the (in)accuracy of energy estimation, caused by the uncertainty of vehicle and

environmental parameters. The parameters with the highest impact are identified and it is recommended to determine them exactly, in order to achieve the estimation accuracy required by the application.

Furthermore, we prioritize parameters according to their impact on estimation accuracy. This is important because fixing a parameter value means putting effort into determining its true value, e.g. by measuring it or requesting it from the driver. Also for calibrating an LDM (e.g. for estimating energy demand for a trajectory of a BEV), the performance of the calibration process regarding computational effort and accuracy can be increased by calibrating only the most influencing factors as proposed by the sensitivity analysis. When estimating a driving range, the accuracy of energy demand estimation is related to the probability of running out of energy while driving. By knowing the uncertainty of the estimated energy demand, the minimum driving range at a given probability can be estimated. Therefore, the information about the uncertainty of energy demand estimation leads to a more reliable driving range estimation.

3. Sensitivity Analysis

Sensitivity analysis is a method to study how uncertainty in the model inputs affects the model response (Campolongo et al., 2011). It describes the relative importance of each input factor in determining variability of model response. According to Saltelli et al. (2004) there are four main settings for conducting a sensitivity analysis:

- Factor prioritization aims at ranking factors according to the reduction of output variance, which could be achieved knowing the true value of the factor.
- Factor fixing aims at identifying factors having no influence on the output and which therefore can be set to an arbitrary value within a predefined range.
- Variance cutting aims at identifying a subset of factors to be fixed in order to achieve a predefined reduction of variance of the model output.
- Factor mapping aims at identifying factors mostly responsible for causing a realization in a predefined region of the output.

This study focuses on factor prioritization, i.e. which parameters have to be chosen carefully to obtain a realistic energy demand estimation. Based on this ranking, variance cutting is performed to achieve a desired variance for our energy estimation. Prior to the sensitivity analysis, ranges for the factors have to be defined, which represent the uncertainty encountered in reality. Increasing the uncertainty of a parameter will increase the output variance. Therefore, the uncertainty range for each parameter has to be defined carefully.

3.1. Sobol's Sensitivity Index

Two important sensitivity indices are frequently used for sensitivity analysis (Saltelli et al., 2004): The first-order sensitivity index (SI) is equal to the first-order effect of each factor normalized by the total variance, and it can be

interpreted as the portion of the output variance that is due only to the variation of one input factor. This indicator captures the "stand-alone" effect of the input factor on the model output. Assuming a set of vectors $(X_1, X_2, ..., X_n)$ representing the input factors of the model, then the SI of parameter i can be computed as

$$SI_i = \frac{V(E(Y|X_i))}{V(Y)}, \tag{9}$$

where V is the variance, E the expectation value and Y represents the model response. For parameter i, the expectation value of the model output, given the variation of all parameters but i, is estimated. The variance of this expectation value is estimated for all values of X_i and normalized by the total variance.

For non-additive models, the interaction of each factor with some or all of the input factors may influence output variance, referred to as interaction (or higher order) effect related to each factor. The total sensitivity index (TSI) is the sum of the first-order effect of each factor and of all the higher order effects that involve this factor, normalized by the total variance. The sum of the first-order and higher order effects for all the input factors explains the total output variance. The TSI for parameter i is calculated by

$$TSI_i = \frac{E(V(Y|X_{-i}))}{V(Y)}, \tag{10}$$

where X_{-i} means that all parameters except i are fixed. To calculate the TSI, the output variance is estimated for different values of X_i. The expectation value of this variance over all values of X_i is then normalized by the total variance. It is important to consider whether the investigated factors are independent respectively orthogonal. As the model parameters can be considered as independent from each other, sensitivity analysis can focus on the interactions of factors. One pair of known interacting factors is basic energy demand and average vehicle speed (cf. Figure 6).

3.2. Parameters of the Longitudinal Dynamics Model

The LDM, as described in Section 2.1, contains eleven parameters. Parameter values may vary for different trips or even within a trip and are not always easily accessible (e.g. total weight, efficiency). Subsequently, the uncertainty range of each parameter is discussed based on literature and measurements from a BEV (Mitsubishi i-MiEV). This vehicle represents an average BEV and many parameters are similar or equal in other passenger cars. Moreover, the uncertainty of parameters is expected to be in the same magnitude for common passenger BEVs.

1. **Efficiency of driving (η_M):** The power to accelerate has to be provided by the drive train of the vehicle. A simplified illustration of the drive train of a BEV is presented in Figure 2.
   Each component of the drive train has a certain efficiency, of which some vary with power and/or speed. Total efficiency of the drive train is the product of efficiency of the battery $\eta_{battery}$, power electronics $\eta_{electronic}$, electric motor η_{motor} and transmission $\eta_{transmission}$. Losses of the battery are caused by the internal resistance and increase with power. For a lithium ion battery and a power up to 50 kW, efficiency varies between

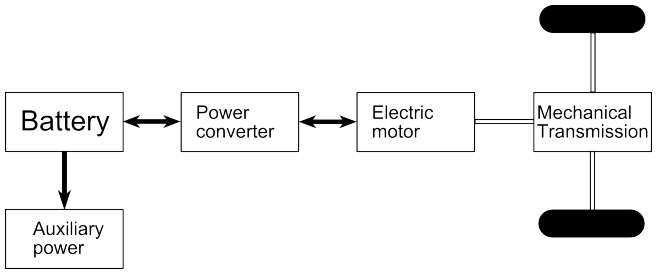

Figure 2: Drive train of a BEV.

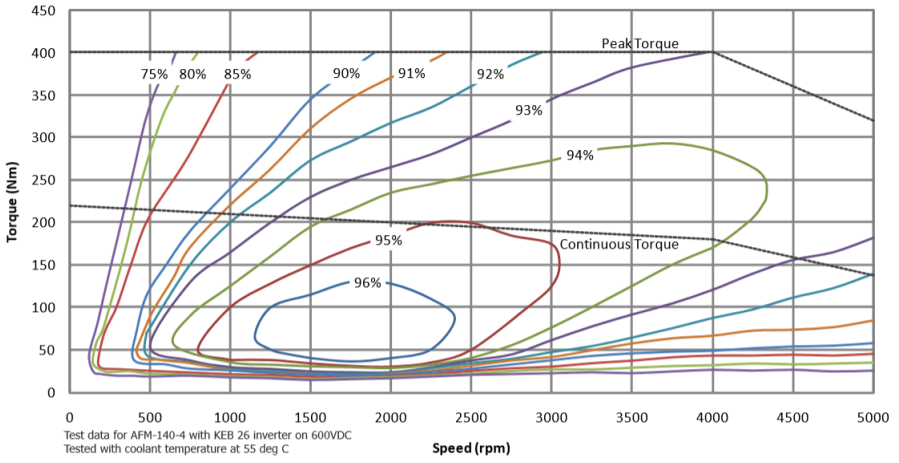

Figure 3: Performance map of an electric motor (EVO Electric, 2014).

0.99 and 0.95 (Koehler et al., 2012). The power converter is responsible for converting direct current (DC) of the battery to alternating current (AC) for the electric motor. Nowadays, converters achieve high efficiencies of 0.98 over a wide load range (Hayes et al., 2011). The highest variability of drive train efficiency is caused by the electric motor. In Figure 3, the performance map of a synchronous motor with permanent magnets, as used in electric vehicles, is presented. The map shows that an electric motor is able to work at an efficiency of up to 0.96. For a large range of rotational speeds and torque, the efficiency does not fall below 0.75. Thus, in our study, we assume the efficiency of the electric motor to be between 0.75 and 0.96.

Finally, the efficiency of a single gear transmission is above 0.97 for a wide rotational speed range (Hayes et al., 2011). Efficiency of the drive train is the product of efficiencies of individual components and therefore η_M varies between 0.63 and 0.9 (considering individual variations).

2. **Efficiency of recuperating (η_G):** In case a negative torque is acting on the wheels of the vehicle, the electric motor is working as a generator and is producing electric energy. Thus, energy is flowing in the opposite direction compared to driving. Again total efficiency is the product of efficiency of each component of the drive train. The efficiency of the transmission is approximately 0.97, as indicated by Hayes et al. (2011).

The efficiency map of an electric motor in generator mode is almost identical to driving mode (cf. Schwingshackl, 2009). So the efficiency range of the electric motor is defined equally for both operational modes (0.75 to 0.96). During recuperation, the power electronic is converting AC to DC, which can be done at high efficiency (0.98). During recuperation, electric energy is transmitted back to the battery and therefore charging losses have to be considered. According to Hayes et al. (2011), efficiency of an on-board charger is 0.9. Therefore, total efficiency of the drive train during recuperation η_G, which is the product of individual efficiencies, is within in the range of 0.64 to 0.82.

3. **Total mass (m):** The total mass is composed of the curb weight, weight of the driver, passengers and additional payload (e.g. luggage). The vehicle mass is well described in technical specifications of the BEV and does not vary during a trip. At least the weight of one driver has to be added to the vehicle mass, for which a minimum value of approximately 60 kg can be assumed. Most BEVs offer seats for four passengers and therefore, the total mass may be significantly higher than the vehicle mass. The curb weight of the Mitsubishi i-MiEV is 1085 kg and we assume that the occupation of the vehicle varies between one light driver and a normal driver plus three passengers, each with an average weight of 80 kg (but no payload). Therefore, the variation of total weight is in the range of 1145 kg to 1405 kg.
4. **Mass factor (f):** A BEV also consists of rotating parts (motor, transmission, wheels), whose rotational inertia has to be considered. Since the exact mass and dimension of these rotational parts is unknown or difficult to determine, the mass is multiplied by a constant factor greater one. According to Ehsani et al. (2009) or Maia et al. (2011), the mass factor is 1.05. In other studies the mass factor is not considered at all (cf. Nandi et al., 2015). Therefore we assume the mass factor in the range of 1.0 to 1.05
5. **Gravitational acceleration (g):** Gravity is an attraction force between two masses (earth and vehicle) and depends on mass and distance. The gravitational acceleration on the earth surface varies between $9.76\frac{m}{s^2}$ (Nevado Huascaran mountain, Peru) and $9.83\frac{m}{s^2}$ (Arctic ocean)(Hirt et al., 2013). In our study, we assume a BEV operating in a limited area and therefore a constant value of $9.81\frac{m}{s^2}$ is used.
6. **Rolling friction coefficient (c_{rr}):** This coefficient depends on properties of the tires and the road surface. Hysteresis effects during deformation of the tire, when rolling on a hard surface, cause an opposing force (Ehsani et al., 2009). The deformation depends on the type of tires, inflating pressure and temperature. The rolling resistance is further influenced by the macro texture of the asphalt and the velocity of the vehicle (Bosch, 1996; Ehsani et al., 2009). The rolling friction coefficient is difficult to measure and a standardized method has not been established. Researchers assume different values for c_{rr} ranging from 0.005 (Maia et al., 2011) to 0.015 (Demir et al., 2011). According to a study of the Transportation Research Board (National Research Council, 2006), a rolling friction coefficient between 0.007 and 0.014 can be assumed for most passenger cars. This range is applied in our study and conforms well with values given in the automotive handbook by Bosch (Bosch, 1996), a frequently cited

reference on this issue.

7. **Air density (ρ):** The resistance of a body moving in a fluid depends on the density of the fluent and is measured in mass per unit volume. For BEVs, air density is relevant to determine the air drag and depends on temperature, pressure (confirms to altitude) and humidity (NASA, 1954). Applications for calculating the air density (e.g. DeNysschen, 2015) based on altitude, temperature and humidity can be found on-line. For our BEV trips we observe altitudes in the range of 100 to 700 m above sea level and a temperature between -5°and 30°Celsius. For these ranges, air density may vary between 1.055 and 1.296 $\frac{kg}{m^3}$. We assume 70% humidity but it has, however, only a small influence on air density. For example, increasing humidity from 50% to 100% would change air density by less than one percent.
8. **Air drag coefficient (c_w):** This vehicle specific constant depends on the shape of the vehicle. The c_w of current cars ranges between 0.24 (Tesla model S) and 0.38 (Subaru Forester), where lower values equal lower air drag. The air drag coefficient is determined by car manufacturers, where usually a single value for a given vehicle is specified. In contrast, in Hucho (1987) a uncertainty range for the air drag coefficient for different vehicles up to 6% is specified. Moreover, the air drag coefficient does not depend solely on the vehicle shape. For a fully loaded small- to medium-sized car, the angle of attack is changed and increases the air drag coefficient by approximately 2%. Moreover, an opened window increases the air drag coefficient approximately by the same amount (Hucho, 1987). Therefore, in our study, we assume an uncertainty range of 10% from manufacturer specifications. For the i-MiEV a c_w value of 0.35 is specified. Therefore, an uncertainty range between 0.333 and 0.368 is assumed.
9. **Front surface area (A):** The front surface area can be computed as the product of overall width and height of the vehicle, where a certain ground clearance has to subtracted from the height. This is an approximation because vehicle shapes are not ideal rectangles and the front area of the wheels has to be considered as well. Therefore, we assume an uncertainty range of 10% of the front surface area based on the product of width and height minus the ground clearance. Thus, the front surface area for the investigated vehicle varies between 1.81 m^2 and 2.01 m^2.
10. **Auxiliary power demand (P_0):** Additional electric energy is necessary to operate the vehicle, for example, to power the on-board electronics. Depending on environmental conditions (illumination, temperature, etc.) and driver behaviour, extra power is necessary for light, heating, cooling, radio etc. Energy consumption of different consumers and their impact on driving range is described in Geringer (2012) and Benders et al. (2014). In theses studies, an upper bound for auxiliary energy power demand is given (e.g. maximum power of heater), but we are more interested in a realistic range for this parameter. Therefore, we rely on energy consumption measurements from a BEV and define a range which covers 90% of all situations. In Figure 4, we show the frequency of observed values for the auxiliary power demand. The evaluation is based on our recorded BEV data where the required auxiliary power is the measured electric power during stops. Assuming the 5th and 95th percentile as bounds for the uncertainty range, we obtain a minimum of 236W and a maximum of 1266W

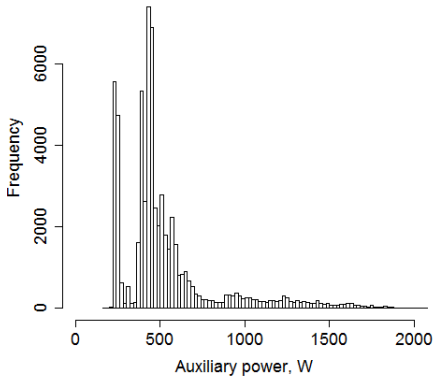

Figure 4: Histogram of observed auxiliary power values.

Nr.	Parameter	Min	Max	Default
1	Efficiency (drive)	0.68	0.9	0.9
2	Efficiency (recuperation)	0.62	0.83	0.8
3	Total mass, Kg	1145	1405	1145
4	Mass factor	1	1.05	1
5	Gravitational acceleration	9.81	9.81	9.81
6	Rolling friction coefficient	0.007	0.014	008
7	Air density, Kg/m^3	1.055	1.296	1.2
8	Air drag coefficient	0.333	0.368	0.35
9	Front surface area, m^2	1.81	2.01	1.9
10	Auxiliary Power, W	236	1266	0.45
11	Minimum speed for recuperation, km/h	0	15	10

Table 1: Uncertainty ranges for parameters of the LDM.

for the auxiliary power demand.

11. **Minimum speed for recuperation (V_{min}):** For a BEV it is not possible to regenerate electric energy during braking at low speeds because of the low electromotive force generated at low motor rotational speeds (Ehsani et al., 2009). For this reason, a minimum speed for recuperation has to be introduced, with no energy being recuperated below this limit. Ehsani et al. (2009) define this limit at 15km/h. In other studies (e.g. Maia et al., 2011), a recuperation is possible for all speeds. Therefore, in our study, we assume the uncertainty range of this parameter between 0 and 15km/h.

Table 1 summarizes the ranges for each parameter as discussed.

4. Trip Database

For the sensitivity analysis in our study we use 1 Hz GPS records from a BEV (Mitsubishi i-MiEV). Rebadged variants of the i-MiEV are also sold as Peugeot

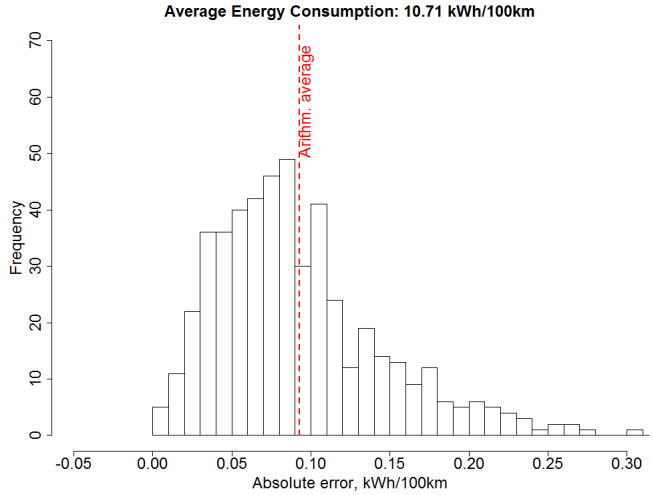

Figure 5: Error distribution of trajectories with 1Hz resolution compared to 10Hz.

iOn and Citroen C-Zero. The driver of the BEV is also the owner and was not instructed regarding the driving style. These data were recorded in the course of his daily activities (e.g. home to work trips) and consist of trips in both urban and rural environments in the area of Vienna, Austria. The trips cover different road categories with speeds up to 130km/h and with different elevation profiles. Since all trips come from the same driver, the driving behaviour is assumed to be consistent. The mileage of trips is obtained by summing up distances between consecutive locations and acceleration is calculated from changes in speed. For the investigated vehicle, the electric power at the output of the battery is measured and used for the analysis.

4.1. Sampling Error

Since locations and velocities are recorded at 1 Hz, the question is how much error is introduced by this sampling rate. Baouche et al. (2013) compare the estimated energy consumption for different aggregation intervals of velocity profiles. As expected, the relative error is decreasing with shorter aggregation intervals (higher resolution). The shortest aggregation interval in Baouche et al. (2013) is 1 minute, resulting in a relative error of 4%. In order to determine whether or not 1 Hz is sufficient, we used simulated vehicle speed profiles. Using the microsimulation tool VISSIM, an urban road network with several intersections is created and trajectories of vehicles are recorded at a sampling rate of 10 Hz. Afterwards, the resolution of each trip is decreased to one measurement per second. For both high and low resolution, data energy consumption is estimated and compared. In Figure 5, we visualize the distribution of deviations between energy consumption estimates with low and high resolution trajectories. The average deviation is below 0.1 kWh/100km, which equals a relative deviation of approximately 0.1%. Therefore, we conclude that increasing the sampling rate to 10 Hz yields no relevant improvements for energy consumption estimation.

4.2. Elevation Data

In contrast to driving cycles, our data contain elevation information and therefore a road gradient α (Eq. (2)) can be calculated. Ignoring this value can significantly increase the error of the energy estimation model as discussed by Graser et al. (2014). Elevation information and thus road gradient can be derived from different data sources using different sampling methods. We use the EU-DEM, which is a digital surface model covering Europe, created in the course of the Copernicus programme funded by the European Union. The data have been released in November 2013 (INSPIRE Forum, 2014) and are provided at a resolution of 25 meters with elevation values stored as floats. EU-DEM is based on SRTM and ASTER GDEM data (European Environment Agency, 2014). It is worth noting that similar resolution data are available globally as well since the U.S. decided to release SRTM data in 30 meter resolution in 2014 (NASA JPL, 2014). DEMs of this resolution provide a sufficiently detailed basis for energy estimation in most settings but Graser et al. (2015) showed that higher resolution DEMs should be used in mountainous regions, since computations based on EU-DEM overestimated energy demand by 20 to 25% compared to a locally available 10 meter DEM in the Alpine test region. There is currently no free global source of DEMs at this level of detail. Elevation values are determined from the DEM for every point of the trajectories using bi-linear interpolation raster sampling which computes the value based on the nearest four raster cell centres. This method is chosen since bi-linear interpolation results in significantly better energy estimation than simple nearest neighbour sampling (Graser et al., 2015). For our trajectories, elevation values between 112 and 670 meters above sea level are observed.

4.3. Trip Selection

Since we analyze sensitivity of the LDM under different conditions, the analysis is applied to individual trips. All GPS records are split into trips with a duration of 10 minutes. In this way, we can structure our trip database into 945 trips with different speed and elevation profiles. Another advantage of shorter trips is that the average velocity is a better approximation of the speed profile than in the case of longer trips. Moreover, trips are still long enough to contain different values of acceleration and deceleration. We use these trips to analyze energy shares (cf. Section 5) and a subset is used to perform the sensitivity analysis. Since the composition of this subset results from our energy share analysis, we describe the selection of the subset at the end of the following section.

5. Energy Shares

Before discussing the sensitivity analysis, we present our findings on the composition of the total energy estimate based on the individual LDM components. When calculating the total energy consumption of a trip, the energy related to each term of the right side of Eq. (2) is determined, as well as the energy required for acceleration (Eq. (1)). Additionally, the efficiency of the drive train (drive and recuperate) is applied to each component. Thus, the required energy for overcoming the grade resistance does not sum up to zero, even if origin and destination of a trip are at the same altitude. Finally, the basic energy demand, which depends on auxiliary power and travel time, is estimated as well.

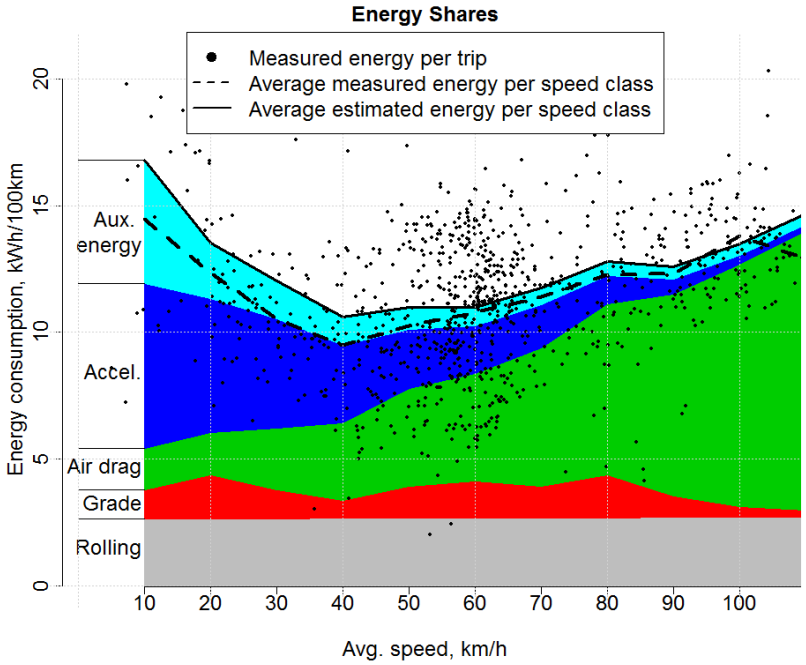

Figure 6: Average energy shares in dependence of average trip speed.

The energy shares are calculated for all 945 trips and an average value for each share and speed category is computed. For the LDM, the default parameters, as listed in Table 1, are assumed. In Figure 6, we present the average energy consumption related to each LDM component over different average trip speeds. Note that, although the length of the trips is varying, energy consumption is always extrapolated to 100km (cf. y-axis in Figure 6).

Figure 6 shows that the air drag is responsible for the majority of energy consumed at high speeds ($>$ 80km/h) but its influence is decreasing for lower speeds. Contrary to the air drag, the energy required for accelerating is dominant at low speeds ($<$ 30km/h), but less important at higher speeds. The same is visible for the auxiliary power, where a relatively low value for P_0 is assumed (cf. Table 1). The energy consumption related to the rolling resistance is constant because it depends only on the distance travelled and we extrapolate trips to 100km.

On average, the energy related to grade resistance is rather low (approx. 10%). As discussed by Graser et al. (2014), significantly larger energy losses can be expected in mountainous regions. To study the influence of elevation, we investigated individual trips using two indicators which are derived from the elevation profile: H_{diff} is the difference in elevation between origin (H_{orig}) and destination (H_{dest}) and is presented in Eq. (11).

$$H_{diff} = H_{orig} - H_{dest} \tag{11}$$

Although origin and destination of a trip are at the same altitude, the elevation profile may vary during a trip. Therefore, the second indicator H_{hilly} is the sum of elevation differences along a trip. From this sum, H_{diff} is subtracted,

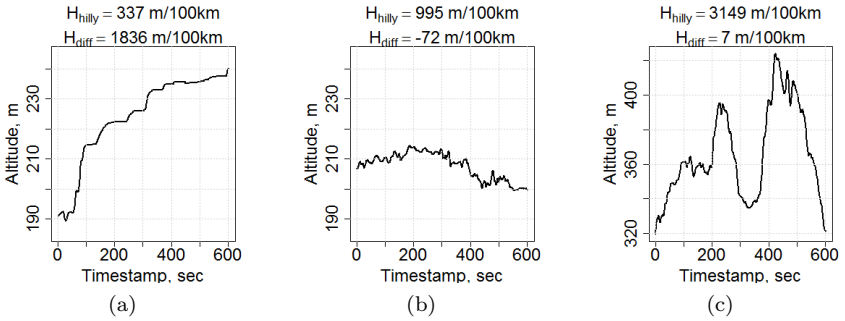

Figure 7: Examples for different elevation profiles.

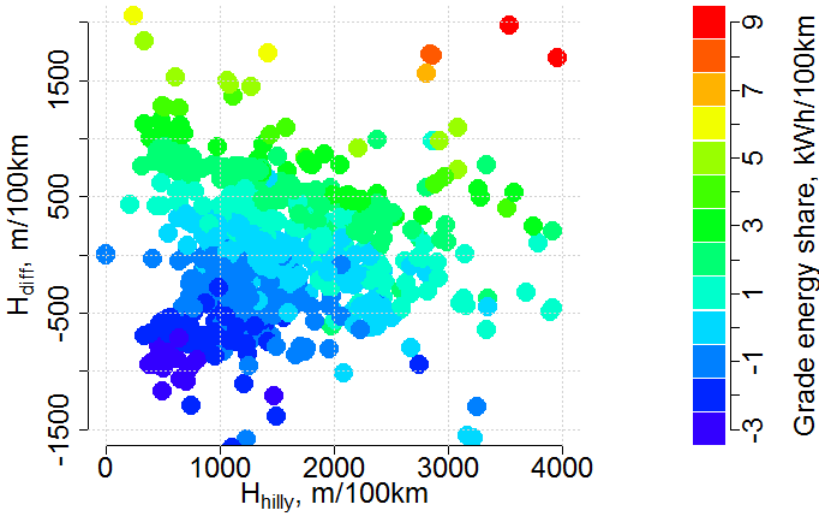

Figure 8: Energy related to grade resistance for different elevation profiles.

in order to obtain an indicator, which is independent of the elevation difference between origin and destination. The calculation is described in Eq. (12), where H_{i+1} is the altitude at the consecutive location along the trip.

$$H_{hilly} = \sum_{i=1}^{N-1} |H_i - H_{i+1}| - |H_{diff}| \tag{12}$$

Figure 7 illustrates these indicators using three examples for different elevation profiles and in Figure 8, we present the energy related to grade resistance for all available trips. Increasing either indicator results in an increased energy demand. The results also show that H_{hilly} has less influence than H_{diff}. The energy consumed for driving uphill is preserved as potential energy and can be recuperated later on, when driving downhill. Although it is not lost, to reach an elevated location, this energy has to be provided by the battery and affects the driving range estimation.

Trip ID	Avg. speed, km/h	Interquartile range, km/h	Avg. acceleration, m/s^2	H_{Diff}, m/100km	H_{Hilly}, m/100km	Description
1	21	[0,41]	0.61	-314	992	small elevation diff.
2	40	[30,52]	0.53	-263	1055	small elevation diff.
3	60	[51,72]	0.37	-11	852	small elevation diff.
4	80	[73,93]	0.45	209	895	small elevation diff.
5	100	[98,102]	0.28	-147	984	small elevation diff.
6	118	[118,118]	0.05	181	547	small elevation diff.
7	80	[67,91]	0.41	46	4410	hilly terrain but small diff. between origin and destination
8	80	[85,90]	0.47	1456	1086	uphill trip
9	80	[69,93]	0.45	-2265	2774	downhill trip

Table 2: Trips used for sensitivity analysis.

This preliminary analysis shows that all components of the LDM have a significant influence on the total energy consumption. If a LDM is used for a specific subset of the road network (e.g. only motorways) and speeds within a restricted range, some of the components can be ignored, including parameters exclusively related to these components. Auxiliary power has less influence for high speeds, because travel time is shorter for the same distance (100km). In our case, we are interested in the sensitivity of each parameter for the complete road network and therefore cannot exclude any parameters a priori .

Since energy shares vary with speed and elevation, this influence has to be considered when performing the sensitivity analysis. The selected trips are described in Table 2 and represent different speed and elevation profiles. To study the influence of speed on sensitivity, trips with different average velocities but similar altitude at origin and destination are selected (first six rows in Table 2). Moreover, all of these trips had comparably small elevation differences along the trip (H_{hilly}). Three more trips are selected for studying only the influence of different elevation profiles and therefore, all of them have the same average velocity. Trip seven has large elevation differences along the route but almost the same altitude at origin and destination. The last two rows of Table 2 represent trips leading uphill (trip eight) and downhill (trip nine). These nine trips cover different speed and elevation profiles and are used to investigate the influence of speed and elevation profile on the sensitivity of the model parameters. Because of the large number of samples of parameter settings (150000), conducting the sensitivity analysis is computationally intensive and therefore we had to limit the number of trips.

6. Sensitivity Analysis Results

In this section, we present the results of the sensitivity analysis of the LDM applied to individual trips with varying speed and elevation profiles. In a first step, the first-order sensitivity index (SI) is calculated and compared to perform a factor prioritization. Afterwards, the total sensitivity index (TSI) is determined and parameters ranked according to their TSI. Based on this ranking, a subset of factors is determined, which has to be fixed, in order to reduce output variance to a predefined limit (variance cutting).

The objective is to identify the influence of the parameters of the LDM on the model output, namely energy consumption per distance unit (Eq. (8)). To calculate Sobol's sensitivity indices (SI and TSI), the model is executed with semi-randomly sampled parameters, within the ranges given in Table 1. For each trip 150,000 parameters settings are chosen in that way and the model output (energy consumption per 100 km) is calculated. Finally Sobol's SI and TSI are calculated according to Eq. (9) and Eq. (10)).

6.1. Factor Prioritization

According to Saltelli et al. (2004), the SI is the proper measure to perform a factor prioritization. A large SI value indicates a high influence of the corresponding parameter on the model output. This implies that this parameter has to be adjusted as accurately as possible, in order to maximize accuracy for energy demand estimation. In contrast, a SI close to zero means that the corresponding factor can be fixed at an arbitrary value within the predefined ranges, without significantly influencing the model response. In Figure 9, we present the SI of each parameter of the LDM for trips with different average speeds but small elevation differences (compare H_{diff} and H_{hilly} in Table 2.

A high influence is visible for efficiency (drive) and rolling friction coefficient for all trip speeds. Auxiliary power also has a large influence, but only for speeds below 80km/h. In general, parameters related to the air drag (air density, air drag coefficient and front area) have a low influence, especially for speeds below 80km/h. However, for higher speeds, the air density gains importance to accurately estimate energy consumption. The influence of recuperation efficiency and total mass is rather small (< 0.1) in this setting. Minimum recuperation speed and mass factor can be ignored at all speeds, since their impact on model results is almost zero. Vertical bars in Figure 9 represent the confidence intervals, since variances are estimated for a limited sample size and therefore deviate from the true variances.

Note that, although factors regarding the air drag (air density, air drag coefficient and front area) have a small influence on the output variance, this does not mean that only little energy is needed to overcome the air drag (as can be seen from Figure 6). It just means that the parameters can be varied within the predefined ranges without significantly changing the energy consumption estimate.

As mentioned in the discussion of the state of the art regarding the LDM (see Section 2.3), velocity and acceleration are suitable indicators to describe driving behaviour. The investigated trips exhibit different speeds and accelerations (cf. Table 2), and therefore we are able to observe the effect of speed and acceleration on the sensitivity of the LDM.

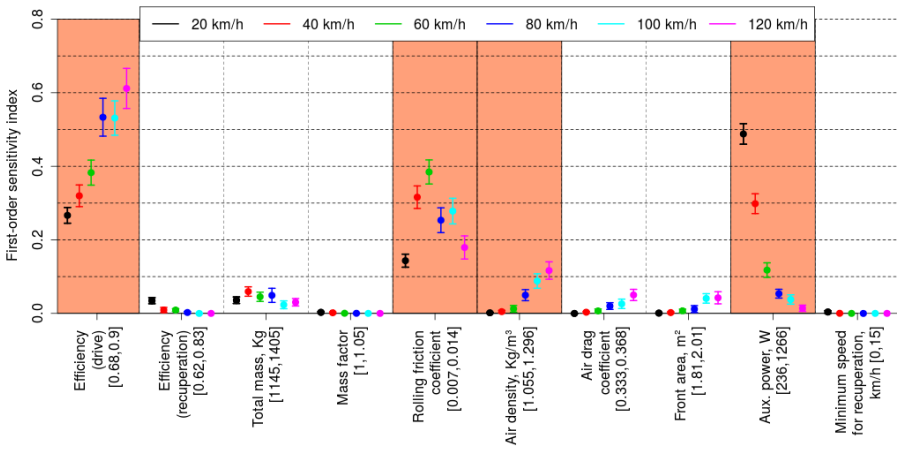

Figure 9: First-order sensitivity index (Eq. (9)) of trips with different velocity. Vertical bars represent 95% confidence intervals. The values in brackets denote the uncertainty range of model parameters.

The velocity chosen by the driver affects air drag and travel time. As mentioned above, SI values of parameters related to the air drag resistance are increasing with increasing speed but are significantly lower compared to the rolling friction coefficient, efficiency or auxiliary power. On the other hand, longer travel times, e.g., caused by a defensive driving style, will increase the effect of auxiliary power consumption on estimation accuracy.

From Eq. (1) we see that acceleration is only related to mass and mass factor. As shown in Figure 9, the sensitivity of the LDM in dependence of these two parameters is rather small and almost constant, although the investigated trips exhibit different average accelerations. Therefore, we conclude that average acceleration as a descriptor of driving behaviour has no influence on the SI of parameters.

The analysis above is performed with trips without elevation differences between origin and destination and only small elevation differences during the trip. To analyze the impact of parameters in a hilly road network, we selected trips with significant elevation differences between origin and destination. Additionally, a trip with no elevation difference between start and end but differences during the trip is analyzed. Details regarding the elevation profile are summarized in Table 2. For all trips, an average trip velocity of 80km/h is measured.

In Figure 10, we present the SI for different elevation profiles. For comparison purposes, the SI of a trip with flat elevation profile and same velocity is plotted as well.

The prioritization of parameters is similar regardless of the elevation profile. Main factors are efficiency (drive) and rolling friction coefficient for all trips. The total mass has a significant impact for trips with varying altitude and/or moving up but can be ignored for trips ending at a lower altitude than their starting position. However, for trips going downward efficiency for recuperation gains importance. For all other parameters the impact on model results nearly is constant for different elevation profiles.

The analysis presented in this section provides a parameter prioritization

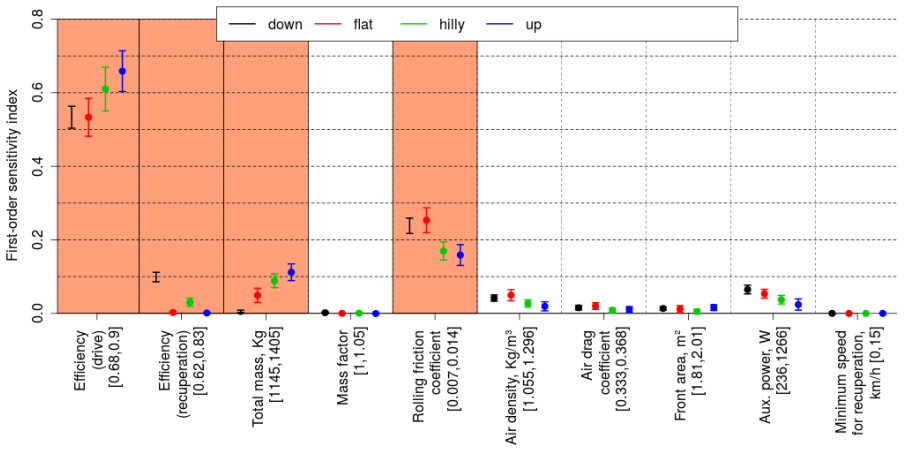

Figure 10: First-order sensitivity index (Eq. (9)) of trips with different elevation profiles. Vertical bars represent 95% confidence intervals. The values in brackets represent uncertainty range of model parameters

with respect to their impact on the accuracy of the energy demand estimation. It has to be emphasized that the SI, represents the share of variance, which is caused by the uncertainty of a parameter. Thus, to determine the (in-)accuracy of the model, the total amount of variance has to be considered as well. Otherwise, a parameter may have a large impact, but due to a small variance this impact is irrelevant. This effect is considered in variance cutting, which we present in the subsequent section.

6.2. Variance Cutting

The aim of variance cutting (VC) is to identify a subset of parameters to be fixed within their uncertainty range, in order to reduce the variance V of the output by a predefined value V_r. In other words, which parameters may be left undetermined while the output variance does not exceed $V - V_r$. This threshold corresponds to the maximum allowed inaccuracy of our model. For example if we define a maximum deviation of 10% given an average energy consumption of 16kWh/100km, we say that in 95% of cases, the energy consumption has to be between 14.4 and 17.6 kWh/100km, corresponding to a standard deviation of 0.8 and a variance of 0.64. If we now reduce our output variance to 0.64 or less, the error of our energy estimation will not exceed 10% (in 95% of the cases). For orthogonal input factors, the following empirical procedure, suggested by Saltelli et al. (2004), is used. We compute the full set of SI and TSI and use the latter to rank the parameters. The ranking refers to the order of variance caused by each parameter. Beginning with the first element (highest TSI), the corresponding variance V_{p_1} is compared to threshold V_r. In case $V_{p_1} > V_r$, we found the parameter to be fixed in order to limit our output variance as desired. Otherwise, the second element of our sequence has to be considered. In case $(V_{p_1} + V_{p_2}) > V_r$, the first two parameters have to be fixed. If this is not the case, the third element is considered and so on. This only works if the model is additive in its factors and they are not interacting. For additive models, the SI of all parameters will sum up to one. As mentioned by Saltelli et al. (2004), it

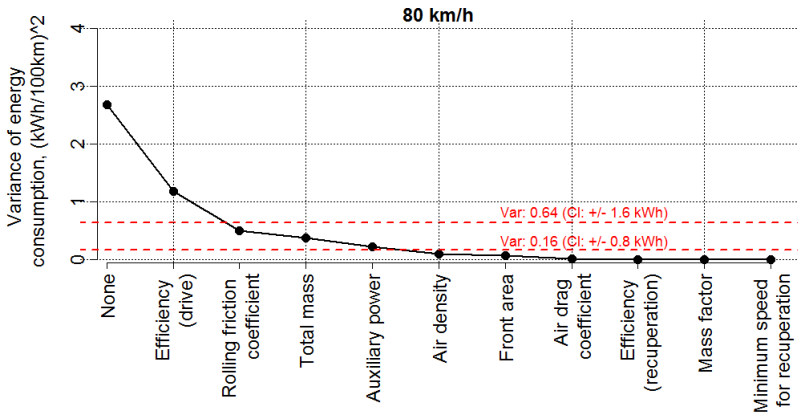

Figure 11: Variance cutting for trip 4 with two different thresholds (red)

is also valid to assume an additive model if experiments show that the sum of SI is 1, even if the analytical formulation shows interactions.

From Table 3, we see that the sum of the SI of the parameters is close to one in all cases and therefore we can assume an additive model. In Table 3, we also listed the output variance V for each trip, which has to be multiplied by the SI of parameter i (see Figure 9 and 10) in order to determine V_{p_i}.

In Figure 11, we present an example for variance cutting. In a first step, all parameters are ranked from left to right according to their TSI. This ranking represents the sequence in which individual parameters are fixed. If no parameter is fixed, then the model has the highest variance (cf. leftmost column in Figure 11), which is the same value as in Table 3 (variance before VC). The largest reduction of variance can be achieved by fixing the parameter with the highest TSI (leftmost parameter), which is the driving efficiency. When this parameter is fixed the variance is reduced by the variance before variance cutting times the TSI (of driving efficiency). If the remaining variance falls below our threshold we have achieved our predefined level of accuracy. Otherwise, we have to fix an additional parameter and further reduce the variance. The choice for the parameter to be fixed next is based on the descending ranking of the TSI. In Figure 11, the decreasing line represents the reduction of variance for factors fixed according to their rank. The dashed lines are the two thresholds which the variance is compared to each time a parameter is fixed. By fixing efficiency (drive) and rolling friction coefficient, the output variance can be reduced to approximately 0.5 and falls below the threshold of 0.64 (red dashed line). If we now reduce the threshold $V - V_r$ to 0.16 (5% error in 95% of the cases), fixing only efficiency (drive) and rolling friction coefficient is not sufficient. Instead, total mass, auxiliary power and air density have to be considered in order to achieve the desired model accuracy.

We repeat the procedure for VC for all trips listed in Table 2 and summarize the results in Table 3. Each row represents the result for one trip. The numbers in the columns associated to the parameters, represent the ranking for VC with a variance threshold of 0.16 (5% error). This means that in order to achieve an error smaller than 5% it is necessary to fix all parameters which are marked by a number in Table 3. If the application allows for a 10% error (threshold of

Trip ID	Parameters										Variance before VC	Variance after VC (Error: 10%, SD/Var: 0.8/0.64)	Variance after VC (Error: 5%, SD/Var: 0.4/0.16)	Sum of SI
	Efficiency (drive)	Rolling friction coef.	Auxiliary power	Total mass	Air density	Efficiency (recup.)	Air drag coef.	Front area	Mass factor	Min. speed (recup.)				
1	2	3	1	5		4					3.961	0.316	0.037	0.98
2	1	2	3	4							2.024	0.164	0.044	1.02
3	1	2	3								1.919	0.381	0.155	0.97
4	1	2	4	3	5						2.689	0.502	0.092	0.97
5	1	2	5		3		4	6			2.801	0.604	0.065	1.03
6	1	2		6	3		5	4			4.581	0.626	0.063	1.04
7	1	2	4	3	5						3.595	0.392	0.16	0.98
8	1	2	5	3	4						4.573	0.324	0.126	1.0
9	1	2	4		5	3					2.185	0.528	0.079	1.01

Table 3: Summary of variance cutting for 5% and 10% (gray) error. Each row represents the result of VC for individual trips. Variance of energy consumption, measured in kWh/100km, is calculated.

0.64), our VC results show that more parameters can be ignored and only those marked with a gray background are necessary. Empty cells indicate that the corresponding parameter is irrelevant to achieve a 10% or 5% error, respectively. In addition to the ranking of parameters, the variance values before and after VC are listed in the columns on the right side of Table 3. For the different trips, the output variance is not constant and is highest for low velocities (trip 1) and high velocities (trip 6). However, the ranking of parameters is similar for different trips. Efficiency (drive) is always the most important parameter, followed by the rolling friction, except for trip 1. For a higher threshold (10% error), auxiliary power is only relevant for trips at low speeds ($\leq$ 40km/h), but it can only be ignored for high speeds (trip 6) in case the lower threshold is applied. Total mass is relevant either for trips in hilly environments or when the lower threshold (5% error) is applied.

Air density has to be considered for speeds $\geq$ 60km/h. Efficiency (recuperation), air drag coefficient and front area have to be considered only if the more restrictive threshold (5% error) is chosen. Finally, the mass factor and minimum speed for recuperation can always be ignored.

7. Conclusions

In our study, we analyze the sensitivity of the energy consumption of a BEV. A literature study reveals that an LDM is widely used, but a detailed analysis of the model parameters and assessment on how the choice of each parameter value affects the model response is missing. The common approach for setting parameter values is to rely on references, but different references suggest quite different values. In a first step, we therefore determine the energy share related to each component of the LDM. The different energy shares depend on velocity and elevation profile. The most energy is consumed at low speeds (due to auxiliary energy demand) and at high speeds (due to the air drag).

In addition, we identify the uncertainty range for each parameter. It represents the range within which the parameter values of a specific vehicle (in our case a Mitsubishi i-MiEV) can vary, since they are unknown or difficult to determine. The accuracy of energy demand estimation for driving this vehicle depends on the uncertainty range.

Furthermore, a SI is calculated to prioritize the influence of parameters on the energy consumption estimation (factor prioritization). This and all other indicators are calculated for selected trips with different average speeds and elevation profiles. Regarding the elevation profile, we distinguish between elevation difference between origin and destination of the trip and elevation differences along the route.

From the analysis we deduce, that regardless of the elevation profile, the most important parameters are efficiency (drive), rolling friction coefficient and auxiliary power demand. Moreover, auxiliary power demand is only relevant for speeds below 80km/h. On the other hand, the air density is only relevant for high speeds (> 100km/h) and the total mass only for trips moving upward and in hilly environments. Finally, efficiency (recuperation) is relevant just for downhill trips.

It has to be emphasized that, although the uncertainty of some parameters has no impact, this does not mean that only little energy is spent on the component related to this parameter (e.g. front surface area is related to the air drag).

Driving behaviour is not considered in detail in our study. It is considered insofar, as the sensitivity analysis is performed for different speeds and average accelerations. The only relevant effect of driving behaviour can be argued for auxiliary power consumption because this parameter gains in importance for larger travel times (due to different driving behaviour).

The results of the factor prioritization help to identify important parameters for calibrating the energy demand estimation. If a large number of parameters has to be calibrated, computational effort and the risk of finding a local optimum is increased. Therefore, a reduced number of parameters can alleviate both problems. To limit the output variance, and thus the model error, variance cutting is performed. Given a maximum error of 10% and 5%, two thresholds for the output variance are defined. Results show that, for all trips, efficiency and rolling friction coefficient have to be fixed to keep the output's variance below the predefined thresholds. For trips with low average speeds (≤ 40km/h), auxiliary power and for high speeds (≥ 120km/h) air density has to be fixed as well. Additionally, hilly environments or trips leading uphill require fixing of the total mass. If a lower maximum error is desired (5%), the subset of param-

eters to be fixed, has to be extended to all parameters, except mass factor and minimum speed for recuperation. However, results from the VC show that the largest reduction of uncertainty can be achieved by determining correct values for efficiency (drive), rolling friction coefficient and auxiliary power demand.

The method described in this study can be used to apply any kind of vehicle energy demand estimation. It helps to decide which factors of the model have to be calibrated more thoroughly and under which circumstances. Moreover, the analysis of energy shares reveals possibilities for reducing the energy consumption, e.g. by driving neither too fast nor too slow.

Based on these results, future research activities should focus on reducing the uncertainty of the drive train efficiency, rolling friction coefficient and auxiliary power demand. For some BEVs models, the efficiency map of the electric motor is available and can be incorporated into the LDM. A model for identifying the rolling friction coefficient depending on the road macro texture and speed is developed in the project MIRAVEC (Haider et al., 2014). Since the macro texture is measurable, this model may be integrated in an enhanced LDM. Furthermore, the constant auxiliary power demand can be replaced by a model with weather conditions as input data.

Acknowledgements

This work is partially funded by the Austrian Federal Ministry for Transport, Innovation and Technology (BMVIT) within the strategic program ERANET Electromobility+ under the grant 832423 (SELECT - Suitable Electromobility for Commercial Transport) and co-funded by the Austrian Climate and Energy Fund (KLiEn) within the strategic programme 'Leuchttürme der Elektromobilität' under the grant 839478 (Crossing Borders).

References

Abousleiman, R., Rawashdeh, O., 2014. Energy-efficient routing for electric vehicles using metaheuristic optimization frameworks, in: Mediterranean Electrotechnical Conference (MELECON), 2014 17th IEEE, pp. 298–304.

Araujo, R.jo, R., Igreja, A., de Castro, R., Araujo, R., 2012. Driving coach: A smartphone application to evaluate driving efficient patterns, in: Intelligent Vehicles Symposium (IV), 2012 IEEE, pp. 1005–1010.

Artmeier, A., Haselmayr, J., Leucker, M., Sachenbacher, M., 2010. The shortest path problem revisited: Optimal routing for electric vehicles, in: Dillmann, R., Beyerer, J., Hanebeck, U., Schultz, T. (Eds.), KI 2010: Advances in Artificial Intelligence. Springer Berlin Heidelberg. volume 6359 of *Lecture Notes in Computer Science*, pp. 309–316.

Baouche, F., Trigui, R., El Faouzi, N.E., Billot, R., 2013. Energy consumption assessment for electric vehicles, in: Proceedings of the International Symposium on Recent Advances in Transport Modelling, p. 5.

Benders, B., Winther, K., Holst, M., Kolf, C., 2014. Green eMotion: Performance validation - Results from EV measurements. Technical Report. Danish Technological Institute.

Bosch, 1996. Automotive Handbook, 4th Ed. Robert Bosch GmbH.

Boubaker, S., Rehimi, F., Kalboussi, A., 2013. Estimating energy consumption of hybrid electric vehicle and gazoline classical vehicle, in: Advanced Logistics and Transport (ICALT), 2013 International Conference on, pp. 221–226.

Campolongo, F., Saltelli, A., Cariboni, J., 2011. From screening to quantitative sensitivity analysis. a unified approach. Computer Physics Communications 182, 978 – 988.

Demir, E., Bekta, T., Laporte, G., 2011. A comparative analysis of several vehicle emission models for road freight transportation. Transportation Research Part D: Transport and Environment 16, 347 – 357.

DeNysschen, 2015. http://www.denysschen.com/catalogue/density.aspx. Accessed: 2015-07-16.

Diaz Alvarez, A., Serradilla Garcia, F., Naranjo, J., Anaya, J., Jimenez, F., 2014. Modeling the driving behavior of electric vehicles using smartphones and neural networks. Intelligent Transportation Systems Magazine, IEEE 6, 44–53.

Ehsani, M., Gao, Y., Emadi, A., 2009. Modern Electric, Hybrid Electric, and Fuel Cell Vehicles: Fundamentals, Theory, and Design, Second Edition (Power Electronics and Applications Series). CRC Press. 2 edition.

European Environment Agency, 2014. Digital elevation model over europe (eu-dem). Http://www.eea.europa.eu/data-and-maps/data/eu-dem, Accessed: 2015-07-16.

EVO Electric, 2014. http://www.evo-electric.com/inc/files/afm-140-spec-sheet-v1.1.pdf. Accessed: 2015-03-16.

Ferreira, J., Monteiro, V., Afonso, J., 2013. Dynamic range prediction for an electric vehicle, in: Electric Vehicle Symposium and Exhibition (EVS27), 2013 World, pp. 1–11.

Frank, R., Castignani, G., Schmitz, R., Engel, T., 2013. A novel eco-driving application to reduce energy consumption of electric vehicles, in: Connected Vehicles and Expo (ICCVE), 2013 International Conference on, pp. 283–288.

Geringer, B., 2012. Fahrzeuge in der Praxis - Kosten, Reichweite, Umwelt, Komfort (Vehicles in Practice - Costs, Range, Environment, Comfort). Technical Report. Österreichischen Vereins für Kraftfahrzeugtechnik.

Goeke, D., Schneider, M., 2015. Routing a mixed fleet of electric and conventional vehicles. European Journal of Operational Research 245, 81–99.

Graser, A., Asamer, J., Dragaschnig, M., 2014. How to reduce range anxiety? the impact of digital elevation model quality on energy estimates for electric vehicles, in: Proceedings of the GI Forum 2014, Austria, pp. 165–174.

Graser, A., Asamer, J., Ponweiser, W., 2015. The elevation factor: Digital elevation model quality and sampling impacts on electric vehicle energy estimation errors, in: 2015 Models and Technologies for Intelligent Transportation Systems (MT-ITS), pp. 1–6.

Haider, M., Kriegisch, M., Benbow, E., Carlson, A., Hammarström, U., Kokot, D., Stryk, J., Adesiyun, A., 2014. Modelling infrastructure influence on road vehicle energy consumption, in: Proceedings of the TRA2014 - Transport Research Arena 2014.

Hayes, J., de Oliveira, R., Vaughan, S., Egan, M., 2011. Simplified electric vehicle power train models and range estimation, in: Vehicle Power and Propulsion Conference (VPPC), 2011 IEEE, pp. 1–5.

Hiermann, G., Puchinger, J., Hartl, R., 2015. The electric fleet size and mix vehicle routing problem with time windows and recharging stations. Technical Report. AIT Austrian Institute of Technology. Working paper, submitted.

Hirt, C., Claessens, S., Fecher, T., Kuhn, M., Pail, R., Rexer, M., 2013. New ultrahigh-resolution picture of earth's gravity field. Geophysical Research Letters 40, 4279–4283.

Hucho, W.H., 1987. Chapter 4 - aerodynamic drag of passenger cars, in: Hucho, W.H. (Ed.), Aerodynamics of Road Vehicles. Butterworth-Heinemann, pp. 106 – 213.

INSPIRE Forum, 2014. EU-DEM and hydrographic network version1 for europe released. Https://inspire-forum.jrc.ec.europa.eu/pg/news/admin/read/238988/eudem-and-hydrographic-network-version1-for-europe-released, Accessed: 2015-07-16.

Kampker, A., Schnettler, A., Vallee, D., 2013. Elektromobilität. Springer, Berlin.

Koehler, S., Viehl, A., Bringmann, O., Rosenstiel, W., 2012. Optimized recuperation strategy for (hybrid) electric vehicles based on intelligent sensors, in: Control, Automation and Systems (ICCAS), 2012 12th International Conference on, pp. 218–223.

Kromer, M.A., Heywood, J.B., 2007. Electric powertrains: Opportunities and challenges in the u.s. light-duty vehicle fleet, in: Pub. No. LFEE 2007-02 RP, Automotive Laboratory, Massachusettes Institute of Technology.

Maia, R., Silva, M., Araujo, R., Nunes, U., 2011. Electric vehicle simulator for energy consumption studies in electric mobility systems, in: Integrated and Sustainable Transportation System (FISTS), 2011 IEEE Forum on, pp. 227–232.

Nandi, A.K., Chakraborty, D., Vaz, W., 2015. Design of a comfortable optimal driving strategy for electric vehicles using multi-objective optimization. Journal of Power Sources 283, 1 – 18.

NASA, 1954. Manual of the ICAO standard atmosphere calculations by the NACA. International Civil Aviation Organization and Langley Aeronautical Laboratory.

NASA JPL, 2014. U.s. releases enhanced shuttle land elevation data. http://www.jpl.nasa.gov/news/news.php?release=2014-321, Accessed: 2015-07-16.

National Research Council, 2006. Tires and Passenger Vehicle Fuel Economy: Informing Consumers, Improving Performance. Transportation Research Board Special Report 286.

Pelletier, S., Jabali, O., Laporte, G., 2014. Goods distribution with electric vehicles: Review and research perspectives. Technical Report. CIRRELT, Montréal, Canada.

Prandtstetter, M., Straub, M., Puchinger, J., 2013. On the way to a multi-modal energy-efficient route, in: Proceedings of the 39th Annual Conference of the IEEE Industrial Electronics Society - IECON 2013, IEEE. pp. 4779–4784.

Preis, H., Frank, S., Nachtigall, K., 2014. Energy-optimized routing of electric vehicles in urban delivery systems, in: Helber, S., Breitner, M., Rsch, D., Schn, C., Graf von der Schulenburg, J.M., Sibbertsen, P., Steinbach, M., Weber, S., Wolter, A. (Eds.), Operations Research Proceedings 2012. Springer International Publishing. Operations Research Proceedings, pp. 583–588.

Sachenbacher, M., Leucker, M., Artmeier, A., Haselmayr, J., 2011. Efficient energy-optimal routing for electric vehicles, in: AAAI Conference on Artificial Intelligence, Special Track on Computational Sustainability, AAAI. AAAI. To appear.

Saltelli, A., Tarantola, S., Campolongon, F., Ratto, M., 2004. Sensitivity Analysis in Practice: A Guide to Assessing Scientific Models. John Wiley & Sons, Ltd.

Schwingshackl, M., 2009. Simulation von Elektrischen Fahrzeugkonzepten fr PKW (Simulation of Electric Vehicle Concepts for Passenger Cars). Ph.D. thesis. Technical University of Graz, Austria.

Sehab, R., Barbedette, B., Chauvin, M., 2011. Electric vehicle drivetrain: Sizing and validation using general and particular mission profiles, in: Mechatronics (ICM), 2011 IEEE International Conference on, pp. 77–83.

Shankar, R., Marco, J., 2013. Method for estimating the energy consumption of electric vehicles and plug-in hybrid electric vehicles under real-world driving conditions. Intelligent Transport Systems, IET 7, 138–150.

Situ, L., 2009. Electric vehicle development: The past, present and future, in: Power Electronics Systems and Applications, 2009. PESA 2009. 3rd International Conference on, pp. 1–3.

Terras, J., Sousa, D., Roque, A., Neves, A., 2011. Simulation of a commercial electric vehicle: Dynamic aspects and performance, in: Power Electronics and Applications (EPE 2011), Proceedings of the 2011-14th European Conference on, pp. 1–10.

Treiber, M., Kesting, A., 2010. Verkehrsdynamik und -simulation: Daten, Modelle und Anwendungen der Verkehrsflussdynamik. Springer-Lehrbuch, Springer Berlin Heidelberg.

Vaz, W., Nandi, A.K., Landers, R.G., Koylu, U.O., 2015. Electric vehicle range prediction for constant speed trip using multi-objective optimization. Journal of Power Sources 275, 435 – 446.

Wu, X., Freese, D., Cabrera, A., Kitch, W.A., 2015. Electric vehicles energy consumption measurement and estimation. Transportation Research Part D: Transport and Environment 34, 52 – 67.

Younes, Z., Boudet, L., Suard, F., Gerard, M., Rioux, R., 2013. Analysis of the main factors influencing the energy consumption of electric vehicles, in: Electric Machines Drives Conference (IEMDC), 2013 IEEE International, pp. 247–253.

Young, K., Wang, C., Wang, L.Y., Strunz, K., 2013. Electric Vehicle Integration into Modern Power Networks. Springer-Verlag New York. chapter Electric Vehicle Battery Technology. pp. 15–56.

Zhang, Y., Wang, W., Kobayashi, Y., Shirai, K., 2012. Remaining driving range estimation of electric vehicle, in: Electric Vehicle Conference (IEVC), 2012 IEEE International, pp. 1–7.